Supplementary Figures and Tables

Figure S1: Correlation matrices (r-value) for the composite record of SAS22-2, SAS21-11 and SAS21-12 for 1 cm resolution data. XRF data were scaled to a 5pt average to account for the noise ratio and different sampling resolution between XRF and other parameters. Only significant values (p ≤ 0.001). Green and red colours indicate positive and negative correlations, respectively.
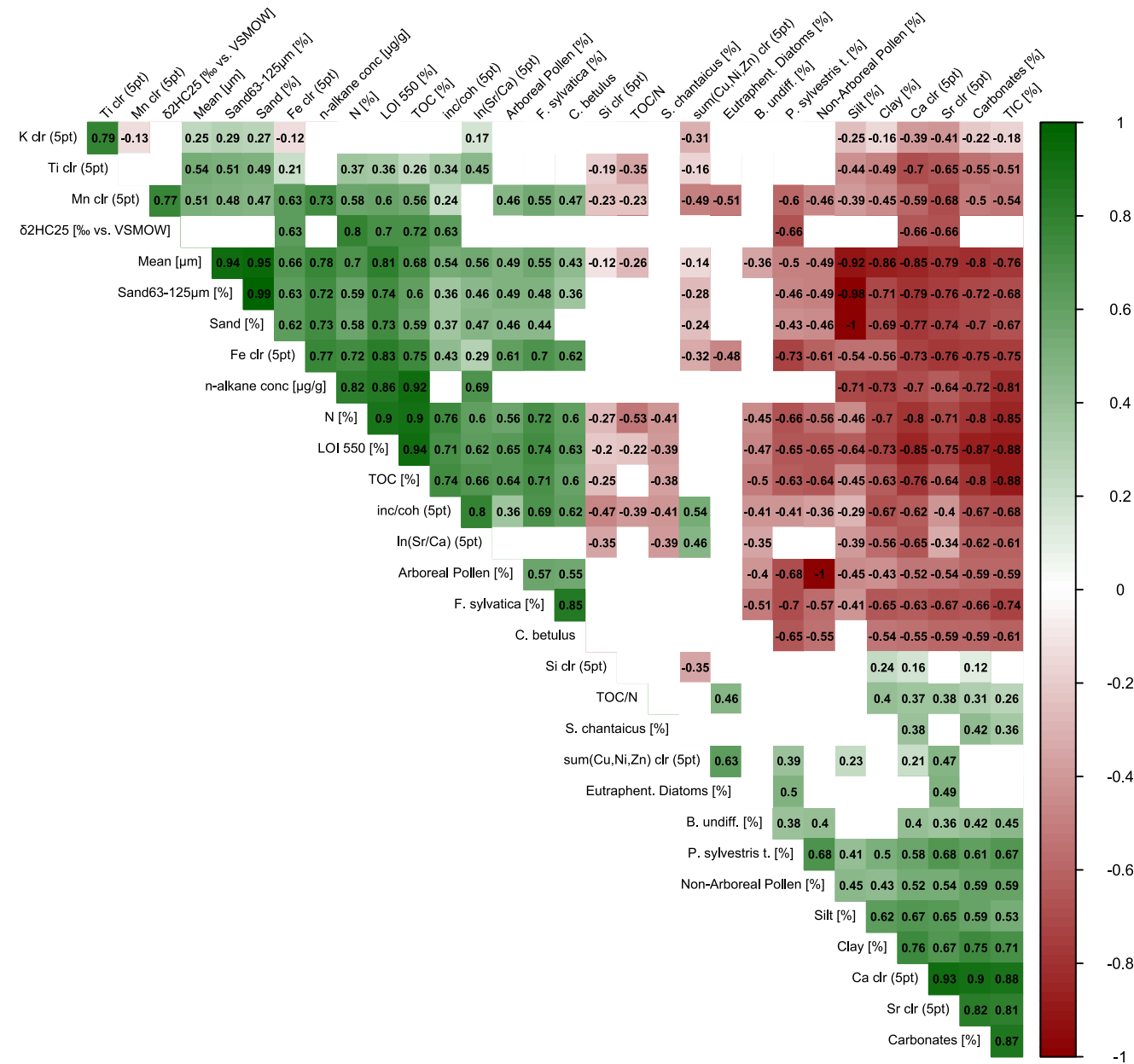
Figure S2: *n*-alkane concentration (C$_{21}$-C$_{35}$), individual concentration of *n*-alkanes (C$_{23}$ – C$_{31}$) available in sufficient amounts for δ^{2}H measurements as well as average chain length (ACL; Poynter et al., 1989), Paq' (Strobel et al., 2021) and odd-over-even predominance (OEP; Hoefs et al., 2002). The compound-specific hydrogen isotopic signature (δ2H) of the n-alkanes C23 – C31 is also shown.
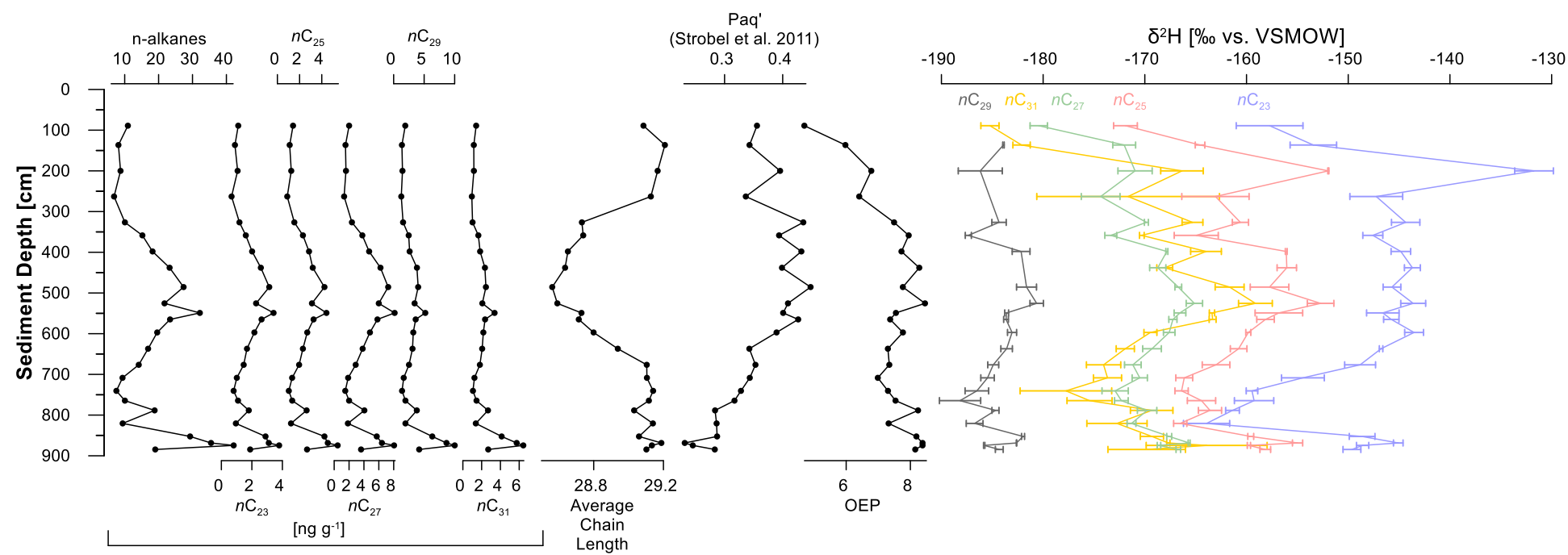
Table S3: Fallout radionuclide concentrations in the Schweriner See sediment core SAS22-2

Depth		^{210}Pb Total		Unsupported		Supported		^{137}Cs	
cm	g cm^{-2}	Bq kg^{-1}	±	Bq kg^{-1}	±	Bq kg^{-1}	±	Bq kg^{-1}	±
0.5	0.1	182.7	9.2	165.0	9.4	17.7	1.8	68.9	1.9
2.5	0.6	147.5	8.4	131.9	8.6	15.6	1.8	70.8	2.0
4.5	1.1	96.4	8.7	80.3	8.9	16.1	1.8	67.0	1.9
8.5	2.0	80.2	6.3	64.5	6.5	15.7	1.4	72.4	1.8
12.5	3.0	92.2	8.5	76.0	8.7	16.2	2.2	76.4	2.4
16.5	3.8	92.4	7.6	80.0	7.8	12.4	1.7	106.9	2.4
20.5	4.6	81.0	7.0	68.1	7.2	12.9	1.6	120.1	2.3
24.5	5.5	83.7	9.6	64.7	9.9	19.0	2.4	169.3	3.1
28.5	6.4	90.3	8.1	70.6	8.3	19.7	1.8	424.7	3.8
32.5	7.3	62.0	9.8	39.0	10.2	23.0	2.9	35.2	2.3
36.5	8.2	65.1	6.3	47.8	6.5	17.3	1.4	38.9	1.6
40.5	9.1	71.6	7.6	55.7	7.7	15.9	1.7	48.5	1.7
44.5	10.0	55.1	8.3	41.2	8.6	13.9	2.1	51.5	2.1
48.5	10.8	39.0	9.8	21.7	10.1	17.2	2.5	24.9	1.9
52.5	11.6	36.8	5.1	19.6	5.3	17.2	1.4	13.9	1.0
56.5	12.5	45.3	9.1	21.6	9.4	23.7	2.2	3.7	1.5
60.5	13.5	46.2	10.8	25.1	11.1	21.1	2.7	1.7	1.7
64.5	14.4	32.3	10.7	14.4	11.1	17.9	3.0	0.0	0.0
68.5	15.4	28.3	10.1	5.5	10.5	22.9	2.7	0.0	0.0

Table S4: Fallout radionuclide concentrations in the Schweriner See sediment core SAS21-11-2

Depth		^{210}Pb Total		Supported		^{137}Cs	
Relative	Absolute						
cm	cm	Bq kg^{-1}	±	Bq kg^{-1}	±	Bq kg-1	±
0.5	57.5	38.3	7.8	20.0	2.0	6.7	1.4
2.5	59.5	54.8	10.5	18.0	2.8	8.9	1.8
7.5	64.5	42.0	9.4	22.7	2.3	4.9	1.7
11.5	68.5	34.1	11.5	19.1	3.1	7.2	2.0

Table S5: ^{210}Pb chronology of the Schweriner See sediment core SAS22-2

Depth		Chronology			Sedimentation Rate		
cm	g cm^{-2}	Date AD	Age y	±	g cm^{-2} y^{-1}	cm y^{-1}	± (%)
0.0	0.00	2022	0	0			
0.5	0.12	2021	1	1	0.15	0.61	10.3
2.5	0.61	2018	4	2	0.17	0.73	12.1
4.5	1.05	2016	6	2	0.24	1.01	12.2
8.5	2.00	2012	10	2	0.25	1.02	13.7
12.5	2.98	2008	14	2	0.21	0.95	14.0
16.5	3.78	2004	18	2	0.18	0.86	13.4
20.5	4.63	1998	24	3	0.16	0.73	15.2
24.5	5.48	1993	29	4	0.14	0.64	18.8
28.5	6.41	1986	36	4	0.15	0.67	19.4
32.5	7.28	1981	41	4	0.19	0.86	18.7
36.5	8.19	1977	45	5	0.19	0.83	18.7
40.5	9.08	1971	51	4	0.13	0.58	18.7
44.5	9.97	1963	59	4	0.12	0.54	18.7
48.5	10.82	1956	66	5	0.12	0.59	18.7
52.5	11.65	1949	73	6	0.11	0.54	18.7
56.5	12.52	1941	81	7	0.08	0.37	18.7
60.5	13.45	1928	94	9	0.06	0.25	18.7
64.5	14.40	1909	113	12	0.06	0.24	18.7

Table S6: Conventional AMS ^{14}C ages for sediment core SAS21. Dating results were obtained from terrestrial macro remains.

Sample Name	Lab ID	Conventional Age [BP]	Error	Depth [cm]
SAS21-11-2 27	Poz-162150	210	30	85
SAS21-11-4 17 cm	Poz-148478	600	30	300
SAS21-12-3 54.5cm	Poz-145372	730	30	312
SAS21-12-4 90cm	Poz-145415	1130	30	397
SAS21-11-6 10 cm	Poz-147404	1320	30	456.5
SAS21-11-6 55 cm	Poz-147405	1470	30	501.5
SAS21-12-6 0 cm	Poz-145232	1560	30	529
SAS21-12-6 54.5cm	Poz-145233	1760	0	583
SAS21-12-6 70.5cm	Poz-145371	1900	35	599
SAS21-12-7 19-19.5cm	Poz-145416	2020	40	669.5
SAS21-12-8 15-15.5cm	Poz-145417	2440	60	777.5
SAS21-12-8 44-45cm	Poz-155010	2545	35	806.5
SAS21-12-9 31-32cm	Poz-154638	3030	30	897.5

References

Hoefs, M. J., Rijpstra, W. C., and Sinninghe Damsté, J. S.: The influence of oxic degradation on the sedimentary biomarker record I: evidence from Madeira Abyssal Plain turbidites, Geochimica et Cosmochimica Acta, 66, 2719–2735, doi:10.1016/S0016-7037(02)00864-5, 2002.

Poynter, J. G., Farrimond, P., Robinson, N., and Eglinton, G.: Aeolian-Derived Higher Plant Lipids in the Marine Sedimentary Record: Links with Palaeoclimate, in: Paleoclimatology and Paleometeorology: Modern and Past Patterns of Global Atmospheric Transport, Springer, Dordrecht, 435–462, 1989.

Strobel, P., Struck, J., Zech, R., and Bliedtner, M.: The spatial distribution of sedimentary compounds and their environmental implications in surface sediments of Lake Khar Nuur (Mongolian Altai), Earth Surf. Process. Landforms, 46, 611–625, doi:10.1002/esp.5049, 2021.